Hydridic Rhenium Nitrosyl Complexes with Pincer-Type PNP Ligands

Aldjia Choualeb,[†] Alan J. Lough,[‡] and Dmitry G. Gusev*,[†]

Department of Chemistry, Wilfrid Laurier University, Waterloo, Ontario N2L 3C5 Canada, and Department of Chemistry, University of Toronto, Toronto, Ontario M5S 3H6, Canada

Received March 6, 2007

The hydride complexes ReHBr(NO)[HN($C_2H_4PR_2$)$_2$] (R = Pr^i, **1a**; Bu^t, **1b**) were synthesized by reactions of [NEt$_4$]$_2$[Re(NO)Br$_5$] with the pincer-type ligands HN($C_2H_4PR_2$)$_2$. Treatment of **1a** and **1b** with Bu^{t}OK led to their dehydrobromination, resulting in the amido hydrides ReH(NO)[N($C_2H_4PR_2$)$_2$] (**2a**,**b**), respectively. The dihydride *trans*-ReH$_2$(NO)[HN($C_2H_4PPr^i_2$)$_2$] (**3a**) was obtained by stirring an ether solution of **2a** under hydrogen. Similarly, partial conversion of **2b** was achieved under hydrogen to give *trans*-ReH$_2$(NO)[HN($C_2H_4PBu^t_2$)$_2$] (**3b**). The structure and properties of complexes **1**−**3** were studied by DFT calculations. Complexes **2a** and **3a** demonstrated low activity for transfer hydrogenation of acetophenone and cyclohexanone due to instability in 2-propanol.

Introduction

Strongly hydridic transition metal hydrides are found in long polarized M−H bonds *trans* to ligands with strong *trans* influence such as H$^-$, NO$^+$, ≡CR, and ≡N.[1] The hydricity is enhanced in the presence of good donor ancillary ligands such as phosphines.[2] One particularly interesting group of hydridic hydrides are those possessing mutually *trans* H$^-$ ligands. Although *trans*-dihydrides are relatively rare compared to the numerous *cis*-dihydride compounds due to the destabilizing influence of the two strong sigma donors,[3] an increasing number of complexes possessing *trans*-hydrides have appeared in the recent literature.[4] Among those, one example was prepared in our laboratory, *mer*-IrH$_3$[HN($C_2H_4PPr^i_2$)$_2$],[5] incorporating a pincer-type PNP ligand and similar to the known complex *mer*-IrH$_3$[HN($SiMe_2CH_2PPh_2$)$_2$] made by Fryzuk and MacNeil.[4x] This complex proved to be an efficient catalyst for transfer hydrogenation of ketones in 2-propanol.[5] The catalytic activity of *mer*-IrH$_3$[HN($C_2H_4PPr^i_2$)$_2$] was thought to be due to the *syn* configuration of the H−N−Ir−H fragment, where the two hydrogen atoms are properly polarized, H$^{\delta+}$···H$^{\delta-}$, for transfer to a carbonyl, in agreement with the mechanism of transition metal-catalyzed transfer hydrogenation.[6] Good hydricity of the catalyst should be important for efficient hydrogenation of polar C═O and C═N bonds; however, the relationship between rates of transfer hydrogenation and hydricity of the catalysts has not been systematically investigated and remains poorly understood. Therefore, we decided to prepare a series of complexes related to *mer*-IrH$_3$[HN($C_2H_4PPr^i_2$)$_2$] in order to correlate their catalytic efficiency with the hydricity of the hydride ligands. In this paper we report the synthesis of *trans*-ReH$_2$(NO)[HN($C_2H_4PPr^i_2$)$_2$] and study its electronic and catalytic properties by computational and experimental means.

Results and Discussion

1. Computational Results. Octahedral complexes ReH$_2$(NO)[HN($C_2H_4PR_2$)$_2$] can exist in several isomeric forms; therefore it was appropriate to investigate structural preferences of this molecule prior to experimental work. In a series of DFT calculations we optimized five isomers of the model system

* Corresponding author. E-mail: dgoussev@wlu.ca.
[†] Wilfrid Laurier University.
[‡] University of Toronto.

(1) (a) Cugny, J.; Schmalle, H. W.; Fox, T.; Blacque, O.; Alfonso, M.; Berke, H. *Eur. J. Inorg. Chem.* **2006**, *540*. (b) Jacobsen, H.; Berke, H. *J. Chem. Soc., Dalton Trans.* **2002**, 3117. (c) Jacobsen, H.; Berke, H. In *Recent Advances in Hydride Chemistry*; Peruzzini, M., Poli, R., Eds.; Elsevier: New York, 2001.

(2) (a) Zhao, Y.; Schmalle, H. W.; Fox, T.; Blacque, O.; Berke, H. *Dalton Trans.* **2005**, 73. (b) Ellis, W. W.; Raebiger, J. W.; Curtis, C. J.; Bruno, J. W.; DuBois, D. L. *J. Am. Chem. Soc.* **2004**, *126*, 2738. (c) Ellis, W. W.; Ciancanelli, R.; Miller, S. M.; Raebiger, J. W.; DuBois, M. R.; DuBois, D. L. *J. Am. Chem. Soc.* **2003**, *125*, 12230. (d) Cheng, T.-Y.; Brunschwig, B. S.; Bullock, R. M. *J. Am. Chem. Soc.* **1998**, *120*, 13121. (e) van der Zeijden, A. A. H.; Berke, H. *Helv. Chim. Acta* **1992**, *75*, 513.

(3) Jordan, R. B. In *Reaction Mechanisms of Inorganic and Organometallic Systems*, 2nd ed.; Oxford University Press: New York, 1998; pp 64−67.

(4) (a) Lee, J.; Pink, M.; Caulton, K. G. *Organometallics* **2006**, *25*, 802. (b) Ben-Ari, E.; Leitus, G.; Shimon, L. J. W.; Milstein, D. *J. Am. Chem. Soc.* **2006**, *128*, 15390. (c) Kloek, S. M.; Heinekey, D. M.; Goldberg, K. I. *Organometallics* **2006**, *25*, 3007. (d) Abbel, R.; Abdur-Rashid, K.; Faatz, M.; Hadzovic, A.; Lough, A. J.; Morris, R. H. *J. Am. Chem. Soc.* **2005**, *127*, 1870. (e) Laporte, C.; Buttner, T.; Ruegger, H.; Geier, J.; Schonberg, H.; Grutzmacher, H. *Inorg. Chim. Acta* **2004**, *357*, 1931. (f) Dahlenburg, L.; Gotz, R. *Inorg. Chim. Acta* **2004**, *357*, 2875. (g) Burling, S.; Mahon, M. F.; Paine, B. M.; Whittlesey, M. K.; Williams, J. M. *Organometallics* **2004**, *23*, 4537. (h) Li, T.; Churlaud, R.; Lough, A. J.; Abdur-Rashid, K.; Morris, R. H. *Organometallics* **2004**, *23*, 6239. (i) Jazzar, R. F. R.; Bhatia, P. H.; Mahon, M. F.; Whittlesey, M. K. *Organometallics* **2003**, *22*, 670. (j) Chatwin, S. L.; Diggle, R. A.; Jazzar, R. F. R.; Macgregor, S. A.; Mahon, M. F.; Whittlesey, M. K. *Inorg. Chem.* **2003**, *42*, 7695. (k) Abdur-Rashid, K.; Clapham, S. E.; Hadzovic, A.; Harvey, J. N.; Lough, A. J.; Morris, R. H. *J. Am. Chem. Soc.* **2002**, *124*, 15104. (l) Abdur-Rashid, K.; Faatz, M.; Lough, A. J.; Morris, R. H. *J. Am. Chem. Soc.* **2001**, *123*, 7473. (m) Li, S.; Hall, M. B. *Organometallics* **1999**, *18*, 5682. (n) Jia, G.; Lau, C. P. *J. Organomet. Chem.* **1998**, *656*, 37. (o) Nemeh, S.; Flesher, R. J.; Gierling, K.; Maichle-Mossmer, C.; Mayer, H. A.; Kaska, W. C. *Organometallics* **1998**, *17*, 2003. (p) Hill, G. S.; Holah, D. G.; Hughes, A. N.; Prokopchuk, E. M. *Inorg. Chim. Acta* **1998**, *278*, 226. (q) Bayse, C. A.; Hall, M. B. *Organometallics* **1998**, *17*, 4861. (r) Rybtchinski, B.; Ben-David, Y.; Milstein, D. *Organometallics* **1997**, *16*, 3786. (s) Desmurs, P.; Visseaux, M.; Baudry, D.; Dormond, A.; Nief, F.; Ricard, L. *Organometallics* **1996**, *15*, 4178. (t) Powell, J.; Horvath, M.; Lough, A. *J. Chem. Soc., Dalton Trans.* **1995**, 2975. (u) Deutsch, P. P.; Eisenberg, R. *Chem. Rev.* **1988**, *88*, 1147. (v) Packett, D. K.; Trogler, W. C. *Inorg. Chem.* **1988**, *27*, 1768. (w) Johnson, C. E.; Eisenberg, R. *J. Am. Chem. Soc.* **1985**, *107*, 3148. (x) Fryzuk, M. D.; MacNeil, P. A. *Organometallics* **1983**, *2*, 682. (y) Brown, J. M.; Dayrit, F. M.; Lightowler, D. *J. Chem. Soc., Chem. Commun.* **1983**, *8*, 414. (z) Goel, R. G.; Ogini, W. O.; Srivastava, R. C. *Organometallics* **1982**, *1*, 819. (aa) Paonessa, R. S. Trogler, W. C. *J. Am. Chem. Soc.* **1982**, *104*, 1138. (bb) Guggenberger, L. J. *Inorg. Chem.* **1973**, *12*, 1317.

10.1021/om070206+ CCC: $37.00
Publication on Web 05/27/2007

Chart 1

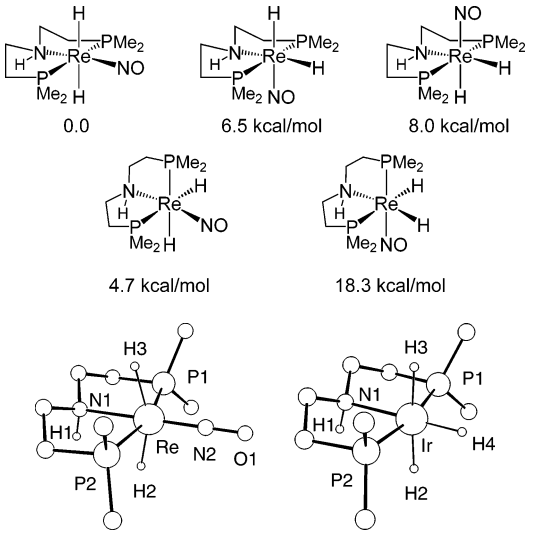

Figure 1. Calculated structures of *trans*-$ReH_2(NO)[HN(C_2H_4PMe_2)_2]$ and *mer*-$IrH_3[HN(C_2H_4PMe_2)_2]$. Unimportant hydrogen atoms are not shown for clarity. Selected distances (Å) and angles (deg): Re−N1 2.289, Re−P 2.360, N1−H1 1.016, Re−N2 1.767, N2−O 1.183, Re−N1−H1 101.4; Ir−N1 2.248, Ir−P 2.258, N1−H1 1.015, Ir−N1−H1 103.3.

$ReH_2(NO)[HN(C_2H_4PMe_2)_2]$ shown in Chart 1. The *trans*-dihydride form of the complex clearly emerged as the most stable, on the basis of the computed enthalpy values. Calculated structures of *trans*-$ReH_2(NO)[HN(C_2H_4PMe_2)_2]$ and *mer*-$IrH_3[HN(C_2H_4PMe_2)_2]$ are presented for comparison in Figure 1. The overall shapes of the two molecules are similar, yet there are some noteworthy differences. Ir−H2 and Ir−H3 bonds are slightly bent away from N1 (∠N1−Ir−H2 = 92.8°), whereas the hydrides on rhenium are bent toward N1 (∠N1−Re−H2 = 78.7°). Therefore, the H1···H2 distance, 2.264 Å, is considerably shorter in the rhenium complex than that in the iridium compound, H1···H2 = 2.651 Å. The distortion in *trans*-$ReH_2(NO)[HN(C_2H_4PMe_2)_2]$ is most probably an electronic effect and serves to increase back-donation to the nitrosyl.[7] For the same reason, the P1−Re−P2 angle is also smaller than the P1−Ir−P2 angle, 161.6° vs 168.0°, respectively. The *trans* M−H2 and M−H3 bonds are relatively long in both complexes (Re−H2 1.738, Re−H3 1.739, Ir−H2 1.673, Ir−H3 1.673 Å), compared to Ir−H4 (1.582 Å) positioned against the nitrogen donor possessing a weak *trans* influence. Re−H bonds are naturally longer than Ir−H bonds, as there is a general trend of longer M−H distances found when moving across the series from late to early transition metals. The differences in Re−H and Ir−H bond distances influence their calculated IR spectra: the asymmetric stretching vibrational frequencies of H2−Re−H3 and H2−Ir−H3 are characteristically very low,[8] 1639 and 1667 cm^{-1}, respectively, compared to ν(Ir−H4) = 2171 cm^{-1}. Corresponding experimental vibrations of hydrides in *mer*-$IrH_3[HN(C_2H_4PPr^i_2)_2]$ and *mer*-$IrH_3[HN(SiMe_2CH_2PPh_2)_2]$ were observed at 1702, 2101 cm^{-1} and 1705, 2175 cm^{-1}, respectively.[4x,5]

Table 1. Calculated Charges on H1−H4 in *trans*-$ReH_2(NO)[HN(C_2H_4PMe_2)_2]$ and *mer*-$IrH_3[HN(C_2H_4PMe_2)_2]$

	ReNH1	ReH2	ReH3	IrNH1	IrH2	IrH3	IrH4
Mulliken	0.302	0.040	0.031	0.294	−0.047	−0.040	0.002
APT	0.144	−0.093	−0.083	0.120	−0.135	−0.128	−0.035
NPA (NBO)	0.399	−0.265	−0.263	0.387	−0.280	−0.279	−0.009

Scheme 1

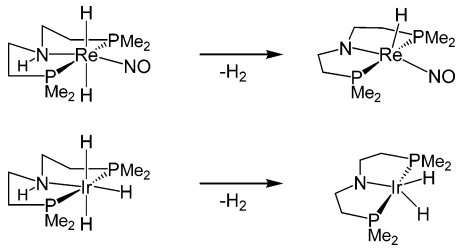

Another important spectroscopic characteristic of *trans*-hydrides is the NMR coupling constant, *trans* ^2J(H−H), which can be twice the magnitude of a regular coupling between *cis*-hydrides, *cis* ^2J(H−H) = 5−7 Hz, and must be negative, although the sign of ^2J(H−H) is usually not available from experiment.[9] Examples of *trans* ^2J(H−H) = 12.5 and 18.2 Hz have been reported for iridium[4e] and ruthenium[10] dihydrides. The calculated *trans* ^2J(H−H) is −16.8 Hz in *trans*-$ReH_2(NO)[HN(C_2H_4PMe_2)_2]$. Confusingly, the iridium trihydrides do not follow this trend. The only observable H−H coupling in *mer*-$IrH_3[HN(C_2H_4PPr^i_2)_2]$ and *mer*-$IrH_3[HN(SiMe_2CH_2PPh_2)_2]$ was *cis* ^2J(H−H) = 5 Hz, and therefore the *trans* ^2J(H−H) coupling should have been very small. The calculated *cis* and *trans* ^2J(H−H) are all between −4.7 and −4.8 Hz in *mer*-$IrH_3[HN(C_2H_4PMe_2)_2]$.

Early transition metal hydrides are typically more hydridic than analogous late transition metal complexes. In the case of *trans*-$ReH_2(NO)[HN(C_2H_4PMe_2)_2]$ and *mer*-$IrH_3[HN(C_2H_4PMe_2)_2]$ it is therefore tempting to assume that the former should be more hydridic, especially considering the formal oxidation numbers, Re(I) and Ir(III). However, the presence of the nitrosyl ligand on rhenium complicates the situation for two reasons. First, NO^+ is an exceptionally strong π-acceptor that should make the metal center relatively electron-poor; second, the reduced H2−Re−H3 angle (156.4° vs 175.0° in the iridium complex) should reduce the degree of *trans*-destabilization and, therefore, polarization of the Re−H bonds. We calculated atomic charges for the hydrides in *trans*-$ReH_2(NO)[HN(C_2H_4PMe_2)_2]$ and *mer*-$IrH_3[HN(C_2H_4PMe_2)_2]$ using three different approaches and summarized the data in Table 1. Ignoring conventional differences between the APT, NPA, and Mulliken charges, we find good internal consistency within each charge definition when comparing the rhenium and iridium hydrides. It appears that IrH2 and IrH3 are more hydridic than ReH2 and ReH3, whereas Ir−H4 can be described as a nonpolar covalent bond. We make this conclusion cautiously, because "hydricity" is a complex property and, like acidity, has specific meanings in the thermodynamic and kinetic senses. Presently, little is known about correlations between the thermodynamic and kinetic hydricities and atomic charges.

An important intermediate in the process of transfer hydrogenation is the dehydrogenated form of the catalyst, such as the amido complexes ReH(NO)[$N(C_2H_4PMe_2)_2$] and $IrH_2[N(C_2H_4$-

(5) Clarke, Z. E.; Maragh, P. T.; Dasgupta, T. P.; Gusev, D. G.; Lough, A. J.; Abdur-Rashid, K. *Organometallics* **2006**, *25*, 4113.

(6) (a) Noyori, R. *Angew. Chem., Int. Ed.* **2002**, *41*, 2008. (b) Clapham, S. E.; Hadzovic, A.; Morris, R. H. *Coord. Chem. Rev.* **2004**, *248*, 2201. (c) Bullock, R. M. *Chem.−Eur. J.* **2004**, *10*, 2366.

(7) Yandulov, D. V.; Huang, D.; Huffman, J. C.; Caulton, K. G. *Inorg. Chem.* **2000**, *39*, 1919.

(8) Adams, D. M. *Metal-Ligand and Related Vibrations*; Edward Arnold (Publishers) Ltd.: London, 1967; p 6.

(9) (a) Gründemann, S.; Limbach, H.-H.; Buntkowsky, G.; Sabo-Etienne, S.; Chaudret, B. *J. Phys. Chem. A* **1999**, *103*, *4752*. (b) Gusev, D. G. *J. Am. Chem. Soc.* **2004**, *126*, 14249.

(10) Bautista, M. T.; Earl, K. A.; Maltby, P. A.; Morris, R. H. *J. Am. Chem. Soc.* **1988**, *110*, 4056.

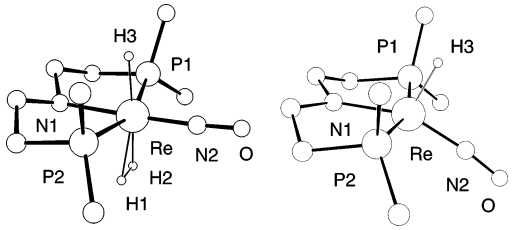

Figure 2. Calculated structures of *trans*-ReH(H_2)(NO)[N(C_2H_4-PMe_2)$_2$] and ReH(NO)[N($C_2H_4PMe_2$)$_2$]. Unimportant hydrogen atoms are not shown for clarity. Selected distances (Å) and angles (deg): (left) Re−N1 2.139, Re−P 2.390, H1−H2 0.89, Re−H3 1.690, Re−N2 1.786, N2−O 1.178, N1−Re−H3 85.1; (right) Re−N1 2.034, Re−P 2.370, Re−H3 1.652, Re−N2 1.785, N2−O 1.184, N1−Re−H3 111.7, N2−Re−H3 93.6, N1−Re−N2 154.6.

Scheme 2

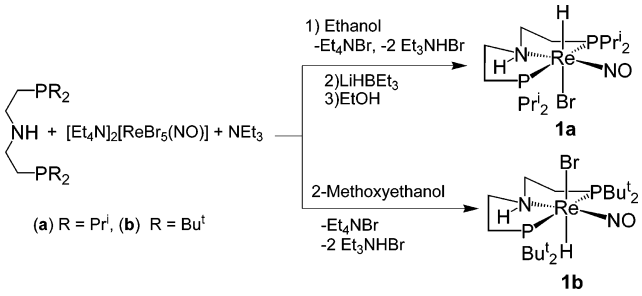

PMe_2)$_2$], which can be derived from *trans*-ReH_2(NO)[HN(C_2H_4-PMe_2)$_2$] and *mer*-IrH_3[HN($C_2H_4PMe_2$)$_2$] according to Scheme 1. DFT calculations revealed that dehydrogenation of the rhenium dihydride is relatively facile, $\Delta H = 11.7$ kcal/mol, and that of the iridium dihydride is thermodynamically less favorable, $\Delta H = 17.8$ kcal/mol. ΔG values for reactions in Scheme 1 must be lower by ca. 6 kcal/mol at room temperature, considering that elimination of H_2 from metal hydrides is entropically favorable by about 20 eu.[11] The calculations also identified the dihydrogen complex *trans*-ReH(H_2)(NO)[N(C_2H_4-PMe_2)$_2$], lying 7.1 kcal/mol above the ground state, as a viable intermediate in the dehydrogenation reaction of *trans*-ReH_2(NO)[HN($C_2H_4PMe_2$)$_2$]. Optimized structures of the rhenium complexes are shown in Figure 2. Noteworthy features of the calculated geometries are (i) flattening of the N1 fragment, reflected in the increasing sum of bond angles around N1 [337.4° (dihydride) < 346.8° (dihydrogen) < 358.3° (monohydride)], and (ii) shortening of the N1−Re bond distance [2.289 Å (dihydride) > 2.139 Å (dihydrogen) > 2.034 Å (monohydride)], following the transformation of the amine complex ReH_2(NO)-[HN($C_2H_4PMe_2$)$_2$] into the amido species ReH(NO)[N(C_2H_4-PMe_2)$_2$].

2. Synthesis of Rhenium Hydrides. Pentabromonitrosylrenate(II), [NEt_4]$_2$[Re(NO)Br_5], is a convenient starting material for preparation of rhenium nitrosyl hydrides.[12] Heating this salt with HN($C_2H_4PPr^i_2$)$_2$ in ethanol gave an orange solid of complex composition that exhibited four single resonances in the ^{31}P NMR spectrum. However, when this mixture was reacted with $LiHBEt_3$ in THF, it cleanly afforded the monohydride ReHBr-(NO)[HN($C_2H_4PPr^i_2$)$_2$] (**1a**) after removal of solvent and trituration in ethanol, according to Scheme 2. Attempts to produce **1a** directly from [NEt_4]$_2$[Re(NO)Br_5] by varying the solvent and heating regime were unsuccessful. However, a related complex, ReHBr(NO)[HN($C_2H_4PBu^t_2$)$_2$] (**1b**), could be prepared by reaction of [NEt_4]$_2$[Re(NO)Br_5] with the ligand HN(C_2H_4-PBu^t_2)$_2$ in 2-methoxyethanol (Scheme 2).

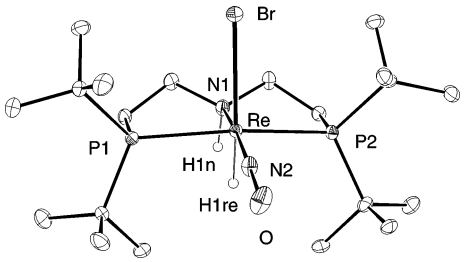

Figure 3. ORTEP and atom-labeling scheme for **1b** with the ellipsoids at 30%. Most of the hydrogen atoms are omitted for clarity. Selected bond distances (Å) and angles (deg): Re−P1 2.4299(15), Re−P2 2.4117(16), Re−N1 2.233(5), Re−N2 1.742-(5), Re−H1re 1.47(5), Re−Br 2.7136(7), O−N2 1.223(6), P2−Re−P1 158.30(5), P1−Re−N1 80.15(13), P1−Re−N2 100.37(17), P1−Re−H1re 83(2), P1−Re−Br 94.02(4), P2−Re−N1 80.81(13), P2−Re−N2 96.03(17), P2−Re−H1re 82(2), P1−Re−Br 95.37-(4), N1−Re−N2 167.7(2), N1−Re−H1re 73(2), N1−Re−Br 87.28-(15), N2−Re−H1re 95(2), N2−Re−Br 104.95(17), H1re−Re−Br 160(2), Re−N2−O 171.8(5).

Complexes **1** were characterized by standard spectroscopic techniques. The IR spectra of **1a** and **1b** showed strong bands at 1655 and 1625 cm^{-1}, respectively, assigned to ν_{NO}. The characteristic vibrations of the N−H and Re−H bonds were observed at 3166 and 1953 cm^{-1} for **1a** and 3192 and 2112 cm^{-1} for **1b**, respectively. The ^{1}H NMR spectra of **1** displayed their hydrides as triplets at δ −5.15 (**1a**) and −4.98 (**1b**). The ^{31}P{^{1}H} NMR spectra of **1a** and **1b** contained singlets due to the equivalent phosphorus nuclei of the molecules.

Both complexes **1a** and **1b** were crystallized and submitted for X-ray analysis; however, a good quality structure was obtained only for the latter. A view of the molecular structure of **1b** is given in Figure 3, and selected bond distances and bond angles are listed in the figure's caption. For **1a**, the X-ray analysis established the arrangement of the ligands around rhenium represented in the structural drawing of Scheme 2. The hydride and bromide ligands are reversed with respect to the PNP plane in **1a** and **1b**; this difference will be addressed below, after a closer look at the crystal structure of **1b**.

The geometry at rhenium in **1b** is close to octahedral with the two *trans* PBu^t_2 groups of the *mer*-PNP ligand adopting an eclipsed conformation, typical of pincer-type ligands with a nonaromatic backbone.[13] The Re−P bonds in **1b** are bent toward the NH, ∠P1−Re−P2 = 158.3°, slightly more than those in the related structure of *cis*-[$ReCl_2$(=NPh)[HN($C_2H_4PPh_2$)$_2$] (∠P1−Re−P2 = 162.3°)[14] presumably due to the influence of the strong π-acceptor NO ligand. The Re−N2 bond distance of 1.742(5) Å and the N2−O distance of 1.223(6) Å lie in the range expected for a linear nitrosyl (∠Re−N2−O = 171.8-(5)°).[15] The hydride of **1b** is *syn* with the N−H bond and *trans* to the bromide. The Re−Br distance, 2.714 Å, is very long in **1b**. Currently, the Cambridge Structural Database contains 452 rhenium complexes with terminal bromides, and only four[16] of these have Re−Br bonds longer than 2.714 Å. In mononuclear complexes, the longest Re−Br bond, 2.795 Å, is found in *cis*-

(11) Hauger, B. E.; Gusev, D. G.; Caulton, K. G. *J. Am. Chem. Soc.* **1994**, *116*, 208.
(12) Gusev, D. G.; Llamazares, A.; Artus, G.; Jacobsen, H.; Berke, H. *Organometallics* **1999**, *18*, 75.
(13) (a) Gusev, D. G.; Lough, A. J. *Organometallics* **2002**, *21*, 5091. (b) Major, Q.; Lough, A. J.; Gusev, D. G. *Organometallics* **2005**, *24*, 2492.
(14) Porchia, M.; Tisato, F.; Refosco, F.; Bolzati, C.; Cavazza-Ceccato, M.; Bandoli, G.; Dolmella, A. *Inorg. Chem.* **2005**, *44*, 4766.
(15) (a) Machura, B. *Coord. Chem. Rev.* **2005**, *249*, 2277. (b) Berke, H.; Burger, P. *Comments Inorg. Chem.* **1994**, *16*, 279.

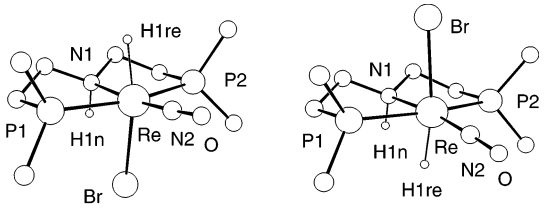

A **B**

Figure 4. Calculated structures of two isomers of ReHBr(NO)-$[HN(C_2H_4PMe_2)_2]$. Unimportant hydrogen atoms are not shown for clarity.

Scheme 3

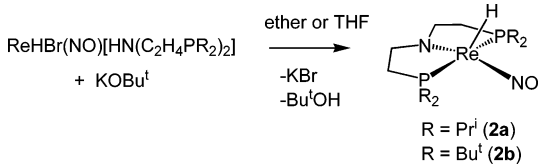

Scheme 4

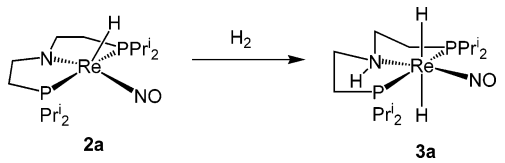

$ReBr_2(\equiv N)(PMe_2Ph)_3$, *trans* to the nitrido ligand; the other Re−Br bond in this complex is normal and much shorter, 2.587 Å.[16b]

To better understand the structural properties of complexes **1a** and **1b**, we calculated two related isomers, **A** and **B**, of the model compound $ReHBr(NO)[HN(C_2H_4PMe_2)_2]$, shown in Figure 4. The Re−Br distances in **A** and **B** are 2.692 and 2.700 Å, respectively, similar to the experimental Re−Br distance in **1b**. Isomer **A** is 2.6 kcal/mol more stable than **B**. Therefore, the structure of **1a** (see Scheme 2) is apparently electronically preferred, whereas the structure of **1b** is different due to the steric constraints imposed by the bulky ligand $HN(C_2H_4PBu^t_2)_2$. We have studied related very bulky pincer-type complexes and have seen the same preference for the bottom axial site to be occupied by the smallest of the coordinated ligands (or no ligand at all).[13] For example, in the dihydrogen complexes $Ru(H_2)Cl_2[O(C_2H_4PR_2)_2]$ the bottom axial site is occupied by a chloride when R = Pr^i and by H_2 when R = Bu^t.[13b]

Treatment of complexes **1** with the strong base potassium *tert*-butoxide led to their dehydrobromination and quantitative formation of the amido complexes $ReH(NO)[N(C_2H_4PR_2)_2]$ (**2**) shown in Scheme 3. Complexes **2a** and **2b** were isolated as dark orange solids crystallized from hexane and toluene, respectively. In the ^{1}H NMR spectra, the hydride ligand was observed as a triplet at δ −10.68 in **2a** and −12.77 in **2b**. The $^{31}P\{^1H\}$ NMR spectra of **2** showed singlets at 80.5 (**2a**) and 96.2 ppm (**2b**), shifted upfield by ca. 30 ppm relative to the corresponding complexes **1**. The NO ligand gave strong bands at 1588 and 1591 cm^{-1} in **2a** and **2b**, respectively, which are shifted to lower wavenumbers relative to **1** due to better back-donation to NO in **2** where the nitrosyl is *trans* to a π-donor amido nitrogen.

(16) (a) Heyen, B. J.; Jennings, J. G.; Powell, G. L.; Roach, W. B.; Thurman, D. W.; Daniels, L. M. *Polyhedron* **2001**, *20*, 783. (b) Schmidt-Brucken, B.; Abram, U. *Z. Anorg. Allg. Chem.* **2001**, *627*, 1714. (c) Moller, A.; Meyer, G. *Z. Anorg. Allg. Chem.* **1993**, *619*, 1655. (d) Aleksandrov, G. G.; Struchkov, Yu. T.; Makarov, Yu. V. *Zh. Strukt. Khim.* **1973**, *14*, 98.

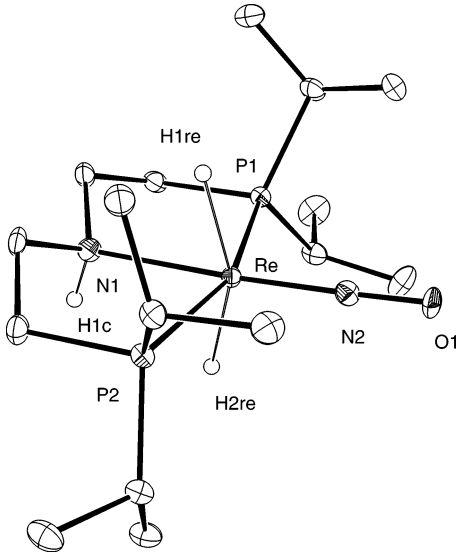

Figure 5. ORTEP and atom-labeling scheme for **3a** with the ellipsoids at 30%. Most of the hydrogen atoms are omitted for clarity. Selected bond distances (Å) and angles (deg): Re−P1 2.3601(13), Re−P2 2.3889(13), Re−N1 2.264(4), Re−N2 1.754-(4), Re−H1re 1.73(5), Re−H2re 1.75(5), O−N2 1.227(5), P2−Re−P1 160.43(4), P1−Re−N1 80.61(11), P1−Re−N2 97.33(14), P1−Re−H1re 89.4(16), P1−Re−H2re 86.1(17), P2−Re−N1 79.83-(11), P2−Re−N2 102.18(14), P2−Re−H1re 85.4(16), P2−Re−H2re 90.7(17), N1−Re−N2 177.29(17), N1−Re−H1re 76.8(16), N1−Re−H2re 78.2(14), N2−Re−H1re 101.5(16), N2−Re−H2re 103.5(14), H1re−Re−H2re 155(2), Re−N2−O 177.7(4).

When an ether solution of **2a** was stirred under hydrogen, *trans*-$ReH_2(NO)[HN(C_2H_4PPr^i_2)_2]$ (**3a**) precipitated as a yellow solid and was isolated in 80% yield (Scheme 4). In solutions of **2b** under hydrogen, only 7% conversion to *trans*-$ReH_2(NO)[HN(C_2H_4PBu^t_2)_2]$ (**3b**) was observed. Formation of **3b** could also be achieved by reaction of **1b** with $LiHBEt_3$. Solutions of complexes **3** in THF and benzene were unstable at room temperature and released hydrogen, regenerating the monohydrides **2**. This process was slow for **3a** (ca. 5% of **2a** formed in 5 min) and relatively fast for **3b**. It is interesting that H_2 addition to **2a** to give **3a** was also slow in solution in contrast to typically very rapid addition of H_2 to effectively unsaturated complexes: the classical example of this reactivity being the immediate formation of the Kubas complex $W(H_2)(CO)_3(PR_3)$ upon saturation of solutions of $W(CO)_3(PR_3)_2$ with hydrogen gas.[17]

Complex **3a** was crystallized and characterized by X-ray diffraction. The crystal structure is shown in Figure 5, and selected bond distances and angles are listed in the figure's caption. It is interesting that the molecules of **3a** form infinite chains in the lattice through the intermolecular NH···ON hydrogen bonds. The first coordination sphere of **3a** is practically the same as that of the calculated model complex *trans*-$ReH_2(NO)[HN(C_2H_4PMe_2)_2]$ discussed in detail in the section devoted to the computational results. In agreement with the solid-state structure, the $^{31}P\{^1H\}$ NMR spectrum of **3a** showed a singlet at 67.2 ppm, and the inequivalent hydrides of **3a** gave rise to doublets of triplets at δ −1.01 and −1.46 in the ^{1}H NMR spectra. The ^2J(HH) = 14.1 Hz was large, as expected for a *trans* dihydride.[4e,10] The IR spectrum of **3a** contained all expected bands due to the N−H, Re−H, and NO stretching

(17) Kubas, G. J. *Metal Dihydrogen and σ-Bond Complexes: Structure, Theory, and Reactivity*; Kluwer Academic/Plenum Publishers: New York, 2001.

Scheme 5

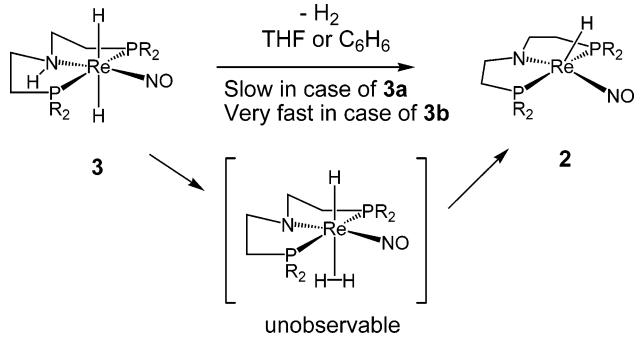

vibrations: 3248 (ν_{NH}), 1858 (ν_{ReH}), 1679 (ν_{NO}), 1570 (ν_{ReH}). The low-frequency asymmetric H−Re−H vibrational band was particularly characteristic and appeared as intense as the NO stretch.

The labile dihydride complex **3b** could not be isolated, and it was characterized in solution by NMR spectroscopy. The ^{1}H NMR spectrum of **3b** exhibited the hydride resonances as two doublets of triplets at δ −0.30 ppm and −0.96 with the *trans* ^2J(HH) = 13.2 Hz. The ^{31}P{^{1}H} NMR spectrum of **3b** showed a singlet at δ 85.6 ppm for the two equivalent phosphorus nuclei. The instability of complexes **3** is interesting and can be explained by a combination of three factors. First is that one of the hydridic Re−H bonds is relatively close to the protic N−H. The second is the availability of a relatively low-energy H_2 elimination pathway through the dihydrogen intermediate *trans*-$ReH(H_2)(NO)[N(C_2H_4PR_2)_2]$ shown in Scheme 5. The related structure of *trans*-$ReH(H_2)(NO)[N(C_2H_4PMe_2)_2]$ in Figure 2 was shown by DFT calculations to be only 7.1 kcal/mol above the ground state, *trans*-$ReH_2(NO)[HN(C_2H_4PMe_2)_2]$. The third factor contributing to the ease of H_2 elimination from **3** is the presence of a π-acceptor NO ligand *trans* to the π-donor amido nitrogen in the product **2**. Therefore, complexes **2** are stabilized by the favorable push−pull interaction of the two ligands through a d_π metal orbital. The relatively high speed at which **3b** decomposes compared to **3a** is a steric effect arising from the greater crowding of $-PBu^t_2$ substituents compared to that of the $-PPr^i_2$ groups.

3. Reactivity and Catalytic Activity of 3a. The hydridic reactivity of **3a** was tested in two conventional experiments: by treating the complex with a protic solvent and by reacting it with CO_2. Rapid evolution of hydrogen gas was observed when **3a** was dissolved in ethanol and 2-propanol. ^{31}P NMR spectra recorded immediately after the sample preparation demonstrated formation of multiple products. The nature of the decomposition of **3a** in alcohols is puzzling considering the possible existence of a stable alkoxide, $ReH(OR)(NO)[HN(C_2H_4PPr^i_2)_2]$, related to the halide complex **1a**.

A room-temperature reaction of **3a** with CO_2 in THF resulted in rapid formation of the formate complex *trans*-$ReH(O_2CH)(NO)[HN(C_2H_4PPr^i_2)_2]$ (**4**) by insertion of CO_2 in one of the two Re−H bonds of **3a**. The reaction was regioselective and the ^{1}H NMR spectrum of the product solution exhibited two hydride resonances at δ −5.80 and −6.05 in a 52:1 ratio, most likely corresponding to the two possible isomers of **4** possessing the hydride ligands *anti* and *syn* with respect to the N−H bond, respectively. The ^{13}C{^{1}H} NMR spectrum of **4** showed a singlet at 173.4 ppm for the carbonyl carbon. The NH and formate CH proton resonances of the main isomer of **4** appeared at δ 8.48 and 7.73 ppm. The characteristically low-field shift of the NH resonance was interpreted as indicative of intramolecular hydrogen bonding in **4** according to Scheme 6. In agreement

Scheme 6

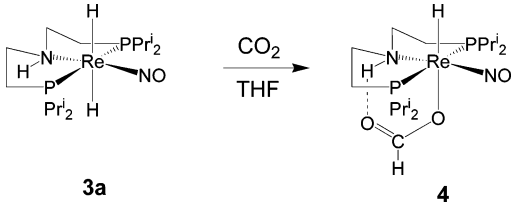

with this, the N−H band was very broad in the IR spectrum of **4**. The presence of the hydride, nitrosyl, and η^1-formate ligands in **4** was also confirmed by the observation of the characteristic bands at 1955(m), 1638 (s), 1590 (s), and 1335 (m) cm^{-1} in the IR spectrum.

We tested catalytic activity of **2a** for transfer hydrogenation at room temperature in an NMR tube reaction of 300 mg of acetophenone in 1 mL of 2-propanol using 6 mg of the catalyst (S/C ratio = 218). Formation of 1-phenylethanol was followed by ^{1}H NMR spectroscopy using 0.3 μs (5°) pulses for quantitative integration of the CH_3 peaks of acetone (δ 2.05) and acetophenone (δ 2.49). A 50% conversion of acetophenone was observed in 1 h, corresponding to TON = 109, and the equilibrium was achieved when conversion reached 66%. Using a similar protocol, we studied transfer hydrogenation of cyclohexanone catalyzed by **3a** (S/C ratio = 300), where 54% conversion was observed in 65 min, corresponding to TON = 162. The ^{31}P NMR spectra of the reaction solutions exhibited multiple peaks in the 40 to 60 ppm range. There was no observable peak of **3a** at ca. 67 ppm and might be only a trace (<1%) of **2a** at ca. 80 ppm in the phosphorus spectrum of the acetophenone reaction. Therefore, the low TON numbers were probably due to decomposition of **3a** in 2-propanol. Complexes **2a**/**3a** did not catalyze hydrogenation of neat acetophenone under an atmosphere of hydrogen, which could be expected because of the slow rate of H_2 addition to **2a**, and therefore slow regeneration of **3a** in the reaction solution.

Concluding Remarks

In this work we prepared and studied *trans*-dihydrides of rhenium, $ReH_2(NO)[HN(C_2H_4PR_2)_2]$ (R = Pr^i, **3a**; Bu^t, **3b**). The stoichiometric and catalytic reactivities of **3a** are consistent with the hydridic character of the Re−H ligands. For unclear reasons, **3a** is unstable in 2-propanol and the extensive decomposition of this complex makes it a poor transfer hydrogenation catalyst compared to the related iridium trihydride *mer*-$IrH_3[HN(C_2H_4PPr^i_2)_2]$.

Experimental Section

General Considerations. All preparations and manipulations were carried out under hydrogen or argon atmospheres with the use of standard Schlenk and glovebox techniques. All chemicals and anhydrous solvents were supplied by Aldrich. The deuterated solvents were dried and degassed before use. The ligands, $HN(C_2H_4PR_2)_2$,[18] and the complex $[NEt_4]_2[ReBr_5(NO)]$ were prepared as described in the literature.[12] The infrared spectra were obtained on a Perkin-Elmer Spectrum BXII FT IR spectrometer. The NMR spectra were recorded on a Varian Unity Inova 300 spectrometer. Throughout this paper, the apparent coupling of observed virtual triplets (vt) is reported as ^vJ. The elemental analyses were performed by Midwest Microlab, LLC (Indianapolis, IN).

(18) Danopoulos, A. A.; Wills, A. R.; Edwards, P. G. *Polyhedron* **1990**, *9*, 2413.

ReHBr(NO)[HN($C_2H_4PPr^i_2$)$_2$] (1a). A mixture of $[NEt_4]_2$[Re(NO)Br_5] (1.44 g, 1.65 mmol), HN($C_2H_4PPr^i_2$)$_2$ (0.604 g, 1.98 mmol), and NEt_3 (0.417 g, 4.12 mmol) was refluxed at 100 °C in 50 mL of ethanol for 48 h. The volume of solvent was reduced to 15 mL, and then the solid was filtered and washed with 3 × 3 mL of ethanol and dried under vacuum. This yielded 0.734 g of an orange solid. A solution of 0.610 g of this solid in 10 mL of THF was treated with 1.196 g (1.34 mmol) of 1 M $LiHBEt_3$ in THF. The mixture was stirred for 2 h and then evaporated under vacuum. This afforded an oily residue, which crystallized upon trituration for 5 min in 2 mL of ethanol. The product was filtered, washed with 2 × 1.5 mL of ethanol, and dried under vacuum to give a yellow powder of **1a** (0.420 g, 0.692 mmol, 50%). Anal. Calcd for $C_{16}H_{38}BrN_2OP_2Re$ (602.54): C, 31.89; H, 6.36; N, 4.65. Found: C, 31.82; H, 6.37; N, 4.56. IR (KBr, cm^{-1}): 3166 (m, ν_{NH}), 1953 (m, ν_{ReH}), 1655 (vs, ν_{NO}). ^{1}H NMR (CD_2Cl_2): δ 3.22 (m, 2H, NCH_2), 2.98 (m, 2H, PCH), 2.68 (br, 1H, NH), 2.35 (m, 2H, PCH), 2.33 (m, 4H, NCH_2 and CH_2P), 1.69 (m, 2H, CH_2P), 1.42 (dvt, ^3J(HH) = 8.7 Hz, $^v J$(HP) = 7.8 Hz, 6H, CH_3), 1.31 (dvt, ^3J(HH) = 4.5 Hz, $^v J$(HP) = 7.2 Hz, 6H, CH_3), 1.20 (m, 12H, CH_3), −5.15 (t, ^2J(HP) = 15.9 Hz, 1H, ReH). ^{31}P{^{1}H} NMR (CD_2Cl_2): δ 51.5. ^{13}C{^{1}H} NMR (CD_2Cl_2): δ 54.8 (t, $^v J$(CP) = 4.8 Hz, NCH_2), 29.4 (t, $^v J$(CP) = 10.7 Hz, CH), 27.8 (t, $^v J$(CP) = 11.4 Hz, CH), 25.8 (t, $^v J$(CP) = 13.5 Hz, CH_2P), 20.7, 20.1, 18.6, 17.6 (s, CH_3).

ReHBr(NO)[HN($C_2H_4PBu^t_2$)$_2$] (1b). A mixture of $[NEt_4]_2$[Re(NO)Br_5] (1.33 g, 1.52 mmol), HN($C_2H_4PBu^t_2$)$_2$ (0.66 g, 1.82 mmol), and NEt_3 (0.38 g, 3.75 mmol) was heated at 120 °C in 30 mL of 2-methoxymethanol for 24 h. The solution was left for 24 h at room temperature. The precipitated solid was filtered, washed with 3 × 1 mL of ethanol, and dried under vacuum to give **1b** as fine orange crystals (0.59 g, 0.89 mmol, 59%). Single crystals of **1b** were grown from an ethanol solution for X-ray analysis. Complex **1b** is sparingly soluble in common organic solvents. Anal. Calcd for $C_{20}H_{46}BrN_2OP_2Re$ (658.65): C, 36.46; H, 7.04; N, 4.25. Found: C, 36.66; H, 7.01; N, 4.17. IR (KBr, cm^{-1}): 3192 (w, ν_{NH}), 2112 (w, ν_{ReH}), 1625 (vs, ν_{NO}). ^{1}H NMR (THF-d_8): δ 3.13 (br, 2H, NCH), 2.95 (br, H, NH), 2.63 (m, 2H, NCH), 2.15 (m, 2H, CH_2P), 2.03 (m, 2H, CH_2P) 1.54 (18H, CH_3), 1.42 (18H, CH_3), −4.99 (t, ^2J(HP) = 19.4 Hz, 1H, ReH). ^{31}P{^{1}H} NMR (THF-d_8): 65.7.

ReH(NO)[N($C_2H_4PPr^i_2$)$_2$] (2a). $KOBu^t$ (0.044 g, 0.396 mmol) was added to a solution of **1a** (0.2 g, 0.33 mmol) in 10 mL of diethyl ether, and the mixture was stirred for 1 h. Then, the reaction solution was filtered and the solvent evaporated. Extraction with hexane followed by evaporation afforded **2a** as an orange oil (0.134 g, 0.257 mmol, 78%). This oil sublimes at 150−160 °C (0.01 mmHg) without decomposition. We were able to crystallize **2a** from hexane at −30 °C. Anal. Calcd for $C_{16}H_{37}N_2OP_2Re$ (521.63): C, 36.84; H, 7.15; N, 5.37. Found: C, 36.68; H, 7.31; N, 5.29. IR (Nujol, cm^{-1}): 2023 (m, ν_{ReH}), 1588 (vs, ν_{NO}). ^{1}H NMR (C_6D_6): δ 3.18 (m, 2H, NCH_2), 2.82 (m, 2H, NCH_2), 2.26 (m, 2H, CH), 1.84 (m, 2H, CH), 1.66 (m, 4H, CH_2P), 1.29 (dvt, ^3J(HH) = 8.7 Hz, $^v J$(HP) = 7.2 Hz, 6H, CH_3), 1.17 (dvt, ^3J(HH) = 8.7 Hz, $^v J$(HP) = 6.9 Hz, 6H, CH_3), 1.05 (dvt, ^3J(HH) = 6.6 Hz, $^v J$(HP) = 6.9 Hz, 6H, CH_3), 0.96 (dvt ^3J(HH) = 7.2 Hz, $^v J$(HP) = 6.9 Hz, 6H, CH_3), −10.68 (t, ^2J(HP) = 12.5 Hz, 1H, ReH). ^{31}P{^{1}H} NMR (C_6D_6): δ 80.5 (s). ^{13}C{^{1}H} NMR (C_6D_6): δ 68.0 (t, $^v J$(CP) = 8.3 Hz, NCH_2), 28.3 (t, $^v J$(CP) = 13.8 Hz, CH), 27.8 (t, $^v J$(CP) = 12.2 Hz, CH), 25.9 (t, $^v J$(CP) = 10.4 Hz, CH_2P), 19.8 (t, $^v J$(CP) = 2.3 Hz, CH_3), 19.2 (t, $^v J$(CP) = 2.3 Hz, CH_3), 18.6, 18.2 (s, CH_3).

ReH(NO)[N($C_2H_4PBu^t_2$)$_2$] (2b). A mixture of **1b** (0.547 g, 0.83 mmol) and $KOBu^t$ (0.111 g, 0.99 mmol) in 20 mL of THF was stirred for 1 h, then it was filtered and evaporated under vacuum. Extraction of the residue with 10 mL of toluene afforded **2b** as an orange powder (0.47 g, 0.81 mmol, 98%). Anal. Calcd for $C_{20}H_{45}N_2OP_2Re$ (577.74): C, 41.58; H, 7.85; N, 4.85. Found: C, 41.70; H, 8.07; N, 4.48. IR (KBr, cm^{-1}): 2026 (w, ν_{ReH}), 1591 (vs, ν_{NO}). ^{1}H NMR (C_6D_6): δ 3.34 (m, 2H, NCH_2), 2.77 (m, 2H, NCH_2), 1.90 (m, 2H, CH_2P), 1.71 (m, 2H, CH_2P), 1.38 (vt, $^v J$ = 6.3 Hz, 18H, CH_3), 1.33 (vt, $^v J$ = 6.3 Hz, 18H, CH_3), −12.77 (t, ^2J(HP) = 12.0 Hz, 1H, ReH). ^{31}P{^{1}H} NMR (C_6D_6): δ 96.2. ^{13}C{^{1}H} NMR (THF-d_8): δ 68.3 (t, $^v J$(CP) = 8.4 Hz, NCH_2), 39.5 (t, $^v J$(CP) = 9.4 Hz, PC), 37.6 (t, $^v J$(CP) = 9.4 Hz, PC), 30.4 (t, $^v J$(CP) = 2.6 Hz, CH_3), 29.1 (t, $^v J$(CP) = 2.8 Hz, CH_3), 26.2 (t, $^v J$(CP) = 9.9 Hz, CH_2P).

ReH_2(NO)[HN($C_2H_4PPr^i_2$)$_2$] (3a). A mixture of **1a** (0.305 g, 0.503 mmol) and $KOBu^t$ (0.067 g, 0.603 mmol) in 20 mL of ether was stirred for 30 min at room temperature under argon. The reaction solution was filtered and was stirred under H_2 overnight to give a yellow suspension. The solvent was reduced to 8 mL and the solution was filtered. The solid was washed with 2 × 1 mL of cold ether and dried under vacuum to give **3a** (0.211 g, 0.403 mmol, 80%). Anal. Calcd for $C_{16}H_{39}N_2OP_2Re$ (523.65): C, 36.70; H, 7.51; N, 5.35. Found: C, 36.56; H, 7.47; N, 5.25. IR (KBr, cm^{-1}): 3248 (m, ν_{NH}), 1858 (w, ν_{ReH}), 1679 (vs, ν_{NO}), 1570 (vs, ν_{ReH}). ^{1}H NMR (THF-d_8): δ 3.21 (br, 1H, NH), 2.93 (m, 2H, NCH_2), 2.09 (m, 8H, CH and NCH_2), 1.89 (m, 2H, CH_2P), 1.51 (m, 2H, CH_2P), 1.33, 1.29, 1.25 (overlapped, 24H, CH_3), −1.01 (dt, ^2J(HH) = 14.1 Hz, ^2J(HP) = 16.6 Hz, 1H, ReH), −1.46 (dt, ^2J(HH) = 14.1 Hz, ^2J(HP) = 14.4 Hz, 1H, ReH). ^{31}P{^{1}H} NMR (THF-d_8): δ 68.1. ^{13}C{^{1}H} NMR (THF-d_8): δ 56.1 (t, $^v J$(CP) = 5.7 Hz, NCH_2), 32.3 (t, $^v J$(CP) = 12.7 Hz, CH), 29.8 (t, $^v J$(CP) = 12.0 Hz, CH), 28.6 (t, $^v J$(CP) = 11.0 Hz, CH_2P), 20.7, 20.3, 20.0,19.5 (s, CH_3).

ReH_2(NO)[HN($C_2H_4PBu^t_2$)$_2$] (3b). ^{1}H NMR (THF-d_8): δ −0.30 (dt, ^2J(HH) = 13.2 Hz, ^2J(HP) = 13.8 Hz, 1H, ReH), −0.96 (dt, ^2J(HH) = 13.2 Hz, ^2J(HP) = 14.4 Hz, 1H, ReH). ^{31}P{^{1}H} NMR (THF-d_8): δ 85.6.

ReH(OCHO)(NO)[HN($C_2H_4PPr^i_2$)$_2$] (4). A solution of **3a** (0.020 g, 0.038 mmol) in 0.5 mL of THF was frozen in a Young NMR tube. The argon atmosphere was removed; the temperature was increased to −20 °C, and the tube was filled and sealed under 1 bar of CO_2. Formation of **4** took place immediately upon shaking of the tube. IR (KBr, cm^{-1}): 1955 (m, ν_{ReH}), 1638 (s, asym ν_{CO}), 1590 (s, ν_{NO}),1335 (m, sym ν_{CO}). ^{1}H NMR (C_6D_6): δ 9.18 (s, 1H, OCH), 7.93 (br, 1H, NH), 2.64 (m, 2H, NCH_2), 2.19 (m, 2H, CH), 1.88 (m, 4H, CH and NCH_2), 1.64 (m, 4H, CH_2P), 1.42 (dvt, ^3J(HH) = 8.4 Hz, $^v J$(HP) = 7.4 Hz, 6H, CH_3), 1.18 (dvt, ^3J(HH) = 9.3 Hz, $^v J$(HP) = 6.9 Hz, 6H, CH_3), 1.07 (m, 18H, CH_3), −5.63 (t, ^2J(HP) = 15.5 Hz, 1H, ReH). ^{31}P{^{1}H} NMR (C_6D_6): δ 55.7. ^{13}C{^{1}H} NMR (C_6D_6): δ 173.4 (s, CO_2H), 54.1 (t, $^v J$(CP) = 5.3 Hz, NCH_2), 29.2 (t, $^v J$(CP) = 10.9 Hz, CH), 28.4 (t, $^v J$(CP) = 11.2 Hz, CH), 27.2 (t, $^v J$(CP) = 14.2 Hz, CH_2P), 20.1 (overlapped, CH_3), 18.9 (s, CH_3), 17.9 (s, CH_3).

Computational Details. The DFT calculations were carried out using Gaussian 03.[19] All geometries were fully optimized without symmetry or internal coordinate constraints using the MPW1PW91 functional, which included modified Perdew−Wang exchange and Perdew−Wang 91 correlation.[20] The basis set employed in this work included SDD (associated with ECP) for Re and Ir, 6-31g(d, p) for

(19) Frisch, M. J.; Trucks, G. W.; Schlegel, H. B.; Scuseria, G. E.; Robb, M. A.; Cheeseman, J. R.; Montgomery, J. A., Jr.; Vreven, T.; Kudin, K. N.; Burant, J. C.; Millam, J. M.; Iyengar, S. S.; Tomasi, J.; Barone, V.; Mennucci, B.; Cossi, M.; Scalmani, G.; Rega, N.; Petersson, G. A.; Nakatsuji, H.; Hada, M.; Ehara, M.; Toyota, K.; Fukuda, R.; Hasegawa, J.; Ishida, M.; Nakajima, T.; Honda, Y.; Kitao, O.; Nakai, H.; Klene, M.; Li, X.; Knox, J. E.; Hratchian, H. P.; Cross, J. B.; Bakken, V.; Adamo, C.; Jaramillo, J.; Gomperts, R.; Stratmann, R. E.; Yazyev, O.; Austin, A. J.; Cammi, R.; Pomelli, C.; Ochterski, J. W.; Ayala, P. Y.; Morokuma, K.; Voth, G. A.; Salvador, P.; Dannenberg, J. J.; Zakrzewski, V. G.; Dapprich, S.; Daniels, A. D.; Strain, M. C.; Farkas, O.; Malick, D. K.; Rabuck, A. D.; Raghavachari, K.; Foresman, J. B.; Ortiz, J. V.; Cui, Q.; Baboul, A. G.; Clifford, S.; Cioslowski, J.; Stefanov, B. B.; Liu, G.; Liashenko, A.; Piskorz, P.; Komaromi, I.; Martin, R. L.; Fox, D. J.; Keith, T.; Al-Laham, M. A.; Peng, C. Y.; Nanayakkara, A.; Challacombe, M.; Gill, P. M. W.; Johnson, B.; Chen, W.; Wong, M. W.; Gonzalez, C.; Pople, J. A. *Gaussian 03*, Revision B.05; Gaussian, Inc.: Wallingford, CT, 2004.

the CH_2 and CH_3 groups, and 6-311+g(d, p) for the rest of the atoms.[21] The nature of the stationary points was verified by frequency calculations. The calculated ν_{M-H} frequencies were scaled by 0.954. A method implemented in Gaussian 03 was used for the spin−spin coupling calculations.[22]

Acknowledgment. We gratefully acknowledge the Natural Sciences and Engineering Research Council of Canada (NSERC) and the Ontario Government for funding.

Supporting Information Available: CIF files for complexes **1b** and **3a**. This material is available free of charge via the Internet at http://pubs.acs.org.

OM070206+

(20) (a) Adamo, C.; Barone V. *J. Chem. Phys.* **1998**, *108*, 664. (b) Perdew, J. P.; Burke, K.; Wang, Y., *Phys. Rev. B* **1996**, *54*, 16533. (c) Burke K.; Perdew, J. P.; Wang, Y. In *Electronic Density Functional Theory: Recent Progress and New Directions*; Dobson, J. F., Vignale, G., Das, M. P., Eds.; Plenum: New York, 1998.

(21) For more information about basis sets implemented in Gaussian 03 and references see: Frish, A.; Frish, M. J.; Trucks, G. W. *Gaussian 03 User's Reference*; Gaussian, Inc.: Pittsburgh, PA, 2003. The basis sets are also available from the Extensible Computational Chemistry Environment Basis Set Database, which is developed and distributed by the Molecular Science Computing Facility, Environmental and Molecular Sciences Laboratory, which is part of the Pacific Northwest Laboratory, P.O. Box 999, Richland, WA 99352 (www.emsl.pnl.gov/forms/basisform.html).

(22) (a) Helgaker, T.; Watson, M.; Handy, N. C. *J. Chem. Phys.* **2000**, *113*, 9402. (b) Sychrovsky, V.; Grafenstein, J.; Cremer, D. *J. Chem. Phys.* **2000**, *113*, 3530. (c) Barone, V.; Peralta, J. E.; Contreras, R. H.; Snyder, J. P. *J. Phys. Chem. A* **2002**, *106*, 5607.